Moisture performance of silica-paper hybrids in the hygroscopic range

N. BOSSE, L. CZERWENKA, A. ANDRIEU-BRUNSEN, AND N. BISHARA

ABSTRACT: Vapor retarders, crucial in building constructions, are traditionally made from plastic-based materials, raising environmental concerns due to the use of fossil materials. This study explores the potential of functionalized papers, particularly silica-paper hybrids, as sustainable alternatives. This work delves into the moisture properties of sol-gel coated linter papers, considering the water vapor permeability and physisorption behavior following DIN EN ISO 12572 and DIN EN ISO 12571. The study addresses hysteresis, noting the lower hysteresis of mesoporous coatings in comparison to dense coatings and implying benefits in moisture release. Findings underscore the need for a nuanced understanding of coating characteristics and their impact on sorption. In order to better assess the relationship between the coating content of the papers and their specific sorption properties, further investigations, such as the measurement of specific surface properties (e.g., specific surface area), are required.

The findings of the water vapor diffusion resistance measurement study demonstrate a correlation between the observed resistance and the vapor levels. The results show that the water vapor diffusion resistance is elevated at lower vapor levels when compared to higher levels. This particular material behavior is typically employed within the construction industry for the utilization of moisture-variable water vapor retarders. The silica-paper hybrids exhibit a response that indicates the potential for advancement into a moisture-variable water vapor barrier.

Application: This research on silica-paper hybrids is a first step towards the application of paper materials in building construction as moisture regulating layers.

The utilization of paper-based materials has recently witnessed a marked increase in their application in high-tech products. For instance, there are functionalized surfaces that have been employed for diagnostics purposes [1,2], for electrical conductivity [3,4], and as a barrier function [5,6]. Paper possesses the capacity to absorb and transport fluid through capillary forces [7-9]. This process has a substantial influence on the material's mechanical stability. The absorption of fluid by paper can lead to fiber swelling, which can result in delamination of the fibers, and consequently paper degradation, thereby causing stability issues. Presently, paper-based materials are primarily employed in interior construction, such as for the core of indoor doors, furniture, or as insulation materials. The prevailing trend in the field is the utilization of paper-based materials as load-bearing components [10].

Silica-paper hybrids

The functionalization of cellulose paper via sol-gel chemistry enables modification of the paper's wettability and liquid transport properties. Applying dense or mesoporous silica coatings transforms the surface from hydrophilic to water repellent. Adjusting the coating alters wettability and capillary flow, as shown by Dubois et al. [11] and Nau et al. [12]. Mikolei et al. [13] demonstrated that liquid transport depends on the silica coating's structure and amount. Dip coating with thermal treatment enables control over wettability, fiber swelling, and fluid transport in all dimensions, achieving a wettability gradient with four dip steps. Mikolei et al. identify three transport scenarios: (1) liquid flows along and into the fibers, causing swelling; (2) liquid enters fiber cavities without swelling; and (3) liquid moves along fiber surfaces without filling cavities or swelling. Silica coatings control absorption by altering surface area and structure. Mesoporous coatings mimic uncoated linter paper but increase liquid uptake over time due to mesopores. Scenario 2 requires a dense, homogeneous coating that smooths fibers and reduces fibrils, lowering surface area and absorption, with slower liquid movement. Gradual coating yields a mix of Scenario 1 and Scenario 3, with Scenario 3 dominating in high silica regions.

Previous studies [11-16] have shown that silica coatings can significantly modify wettability and liquid transport in paper, but did not systematically investigate vapor diffusion resistance or the suitability as moisture-variable vapor barriers. Given the properties of silica-paper hybrids, they could serve as moisture-variable vapor barriers, which is to be investigated in this work.

Water vapor retarders in building construction

Water vapor barriers are categorized by their s_d-value, which indicates how permeable the material is to water vapor compared to an equivalent thickness of air. The s_d-value can be calculated with:

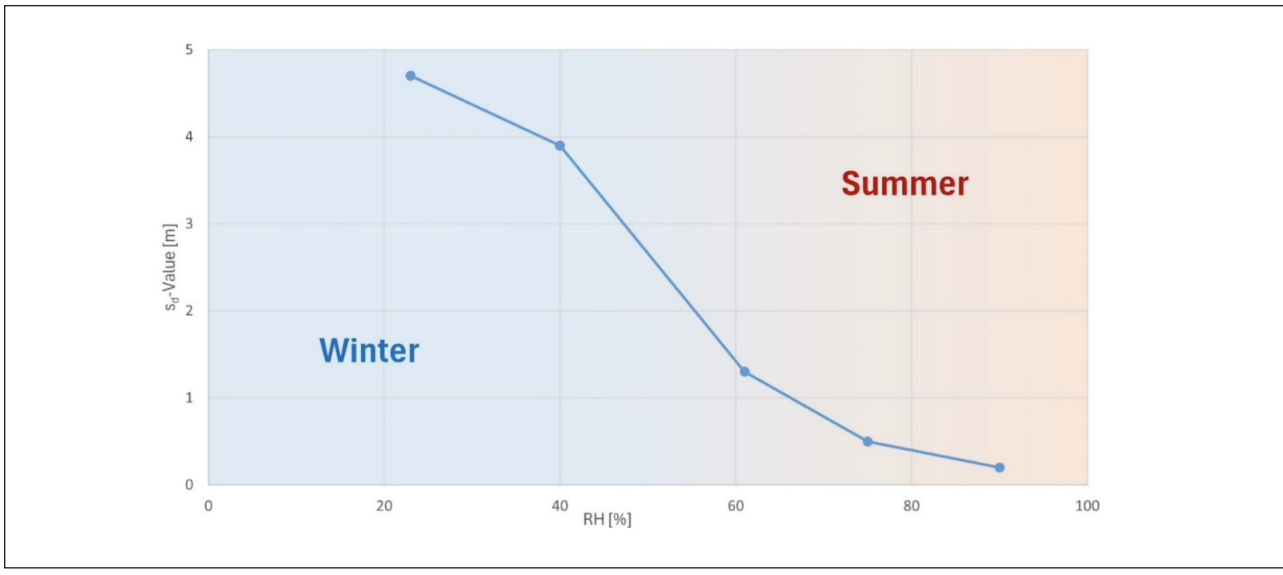

1. Example of an sd-value as a function of relative humidity (RH) for a variable vapor barrier.

$$s_d = \mu \bullet d \quad (1)$$

where:
μ = water vapor diffusion resistance, dimensionless
d = thickness of layer/material, m

Vapor barriers are categorized according to the standard DIN 4108-3:2024-03 "Thermal protection and energy economy in buildings — Part 3: Protection against moisture subject to climate conditions — Requirements, calculation methods and directions for planning and construction" as follows:

- $s_d < 0.5$ m → diffusion open
- 0.5 m < s_d < 1500 m → diffusion inhibiting
- $s_d \geq 1500$ m → diffusion tight

There are two main types of vapor barriers: non-variable and variable. In civil engineering, moisture-variable barriers are increasingly important. Typically made from polymers like polyethylene-copolymer or polyamide, they change water vapor diffusion resistance with relative humidity (RH). This enhances the moisture protection of the building by increasing drying potential, which depends on seasonal vapor flow and barrier placement. The drying potential is influenced by the seasonal changes in the direction of water vapor diffusion and the placement of the vapor barrier within the structure. In winter, water vapor diffuses from the warmer interior to the cooler exterior, while in summer, the direction reverses. **Figure 1** illustrates the relationship between the s_d-value of moisture-variable barriers and RH, demonstrating how material permeability adapts to environmental conditions. The moisture-dependent diffusion resistance is due to the material's pores, which close at low temperatures and vapor pressures and open at higher temperatures and vapor pressures. This dependency is critical for optimizing moisture management in building constructions, as it shows that barriers become more permeable at higher humidity, facilitating drying during summer, and become less permeable at lower humidity, preventing moisture ingress in winter.

As previously noted, commercially available water vapor barriers are typically made from polymers. Both non-variable and moisture-variable vapor barriers generally follow a "cradle-to-grave" life cycle, meaning they are disposed of as waste after use. The Federal Ministry of Housing, Urban Development and Building provides life cycle data for polyethylene (PE) films in the "ÖKOBAUDAT" database [17], covering raw material extraction, transport, production, and disposal, but not transport to, the installation site. Producing PE films consumes significant amounts of total and non-renewable primary energy, contributing to the depletion of these resources, and disposal through incineration leads to further emissions [18,19]. This highlights the potential to reduce emissions and reliance on non-renewable energy. One way to achieve this is by using paper, which is made from renewable and recyclable materials, as a base material instead of plastic. While many plastics are also recyclable, the use of cellulose-based materials offers the added advantage of renewability and often a lower carbon footprint. Recent studies on polymeric vapor barriers (e.g., [20]) have primarily focused on synthetic materials and have not sufficiently addressed the potential of renewable, paper-based systems as sustainable alternatives. Currently, only one moisture-dependent water vapor barrier product on the market contains a significant proportion of paper, but it is bonded to a polyethylene film [21]. Due to adhesives, recyclability is limited, as many paper fibers are lost during separation.

This study investigates silica-coated paper as a sustainable alternative to conventional moisture-variable vapor barriers that face recyclability issues due to polymer layers

and adhesives. We examine whether functionalized paper alone can meet moisture-dependent barrier requirements by analyzing water vapor adsorption, desorption, and diffusion resistance (μ), while addressing the literature gap on vapor transport and providing new data on silica-paper hybrids. The goal is to assess their practical application in civil engineering.

MATERIALS AND METHODS

Paper preparation

In this work, cotton linter paper was used for the coated and uncoated samples. The cotton linter pulp was refined using a Voith LR 40 laboratory refiner (Voith; Heidenheim, Germany) at a specific energy input of 200 kWh/metric ton. Laboratory paper sheets with a grammage of 50 g/m² were then produced from this pulp using a conventional Rapid-Köthen handsheet maker, following standard test methods DIN 54358 "Testing of pulps; preparation of laboratory sheets for physical testing; Rapid-Köthen method" and ISO 5269-2 "Pulps — Preparation of laboratory sheets for physical testing — Part 2: Rapid-Köthen method," without the addition of any additives or fillers.

Mesoporous and dense sol-gel preparation

The coated samples were prepared with dense and mesoporous silica coatings, and uncoated paper was used as a reference. The coatings are based on tetraethoxysilane (TEOS). Three different silica coatings are used in this work: (1) 1:20 TEOS:ethanol (EtOH); (2) 0.5 TEOS; and (3) 0.8 TEOS dense. The addition "dense" in the naming indicates the absence of integrated mesopores in the coating. Coatings without "dense" in the name have integrated mesopores.

To fabricate the silica coatings, the following ratios were used:

1. TEOS was used as the precursor and Pluronic F127 (BASF; Ludwigshafen, Germany) as the micelle-forming template. The solution had the following molar ratios: 1 TEOS : 20 EtOH : 0.05 F127 : 5 H_2O : 0.01 concentrated hydrochloric acid (HCl). This coating is prepared after Mikolei et al. [15].
2. The sol-gel solution was prepared with the precursors TEOS, triethoxymethylsilane (TEMS), and diethoxydimethylsilane (DEDMS), as well as Pluronic F127 in a molar ratio of 0.5 TEOS : 0.3 TEMS : 0.2 DEDMS : 40 EtOH : 0.0075 F127 : 10 H_2O : 0.028 HCl.
3. For this coating, the precursors TEOS, methyltrimethoxysilane (MTMS), and dimethyldimethoxysilane (DMDMS) were used in the following molar ratios: 0.8 TEOS : 0.2 MTMS : 0.08 DMDMS : 40 EtOH : 10 H_2O : 0.028 HCl. The 0.8 TEOS dense coating was prepared after Mikolei et al. [16].

For all sol-gel solution prior to application, the sol-gel solution was stirred at room temperature for 24 h.

The varying precursor compositions result in different functional groups following the sol-gel process. The TEOS undergoes hydrolysis and condensation to form Si-OH groups and Si-O-Si bridges, with the Si-OH groups classified as polar groups in this paper. In contrast, TEMS, DEDMS, MTMS, and DMDMS are considered nonpolar components in this work because they preserve their methyl groups throughout the sol-gel transformation.

Coating preparation

Silica coatings were applied using dip-coating. Cotton linter paper samples (2.5-cm diameter) were used for physisorption tests, and 6.3-cm samples were used for water vapor transmission rate (WVTR) measurements. Samples were immersed in sol-gel solutions at 2 mm/s under a climate of 23°C ± 1°C and 50% ± 5% RH. To generate a mesoporous silica coating, the samples were dipped into a sol-gel solution containing the micelle-forming template Pluronic F127. For a dense silica coating, the same procedure was followed using a sol-gel solution without the template. Mesoporous-coated samples were aged for 1 h after the dipping process, before undergoing thermal treatment. Samples for dense silica coatings skipped the aging step and were subjected directly to thermal post-treatment. Thermal treatment involved heating the samples to 60°C in 10 min, holding for 1 h, then heating to 130°C over 10 min, and holding again for 1 h before cooling to room temperature. Mesoporous samples were finally immersed in acidic ethanol (1M) for three days and dried after at ambient temperature.

Static contact angle

Contact angle measurements were performed using a Model TBU90E from DataPhysics Instruments GmbH (Filderstadt, Germany), along with its associated software on freshly coated samples. For the macroscopic static contact angle analysis and droplet imbibition velocity measurements, a 2-µL water droplet was dispensed onto the thread surface at a rate of 1 µL/s. The imbibition process was recorded on video, from which the static contact angle was measured after 10 s of placing it on the surface. For each coating, three paper samples were prepared, and eight water droplets were placed on each sample to measure the static contact angle. The static contact angles measured for each sample were averaged, and these average values were then further averaged to determine the representative static contact angle for each coating.

Argon gas adsorption-desorption measurements

Argon gas physisorption measurements of unmodified paper samples and dense silica powder were performed using argon gas adsorption at 87 K over a relative pressure range of 0–1, using an Autosorb iQ analyzer (Anton Paar; Ostfildern-Scharnhausen, Germany). Samples with different ages were used for this measurement. The 0.5 TEOS-coated papers were freshly fabricated and compared to

similar samples after two years of storage under ambient climate. From the obtained isotherms, the specific surface area, pore size, and pore size distribution of mesoporous silica-coated paper samples were determined. Prior to each measurement, samples were degassed at 80°C under high vacuum for 12 h. The physisorption isotherms were analyzed using the Brunauer–Emmett–Teller (BET) model (11 points between 0.05 and 0.3 P/P_0) and non-local density functional theory (NLDFT) kernels, processed with the ASiQwin software (Anton Paar).

Dynamic vapor sorption

Dynamic vapor sorption measurement was performed to determine the sorption isotherms of the samples. The measurement was performed with all freshly coated paper samples to assure comparability. To measure the sorption isotherms, the device SPS-1μ Advance from proUmid GmbH & Co. KG (Ulm, Germany) was used. The measurement was based on the standard DIN EN ISO 12571:2022-04 "Hygrothermal performance of building materials and products – Determination of hygroscopic sorption properties (ISO 12571:2021); German version EN ISO 12571:2021," which is commonly used in the building industry to investigate the thermal and moisture behavior of building materials and building products. The parameters described in the standard, such as the weighing interval, have been adapted to the requirements of functionalized papers.

A 15-min weighing interval was set to allow stable measurements and minimize climate disturbances, as climate control is nearly paused during weighing. To account for delayed humidity response, each humidity step lasted at least 75 min. Equilibrium was defined as ±0.01% mass change over 75 min, determined by linear regression. Measurements were conducted at 23°C with RH adjusted in 10% steps from 0 to 90% (adsorption) and back to 0% (desorption). Samples were dried at 23°C and 0% RH within the device before the measurment.

Five samples per coating were tested. For each RH step, the samples were weighed until a constant value was reached (moisture equilibrium). To determine the mass-related moisture content u, the following formula is used:

$$u_i = \frac{m_i - m_0}{m_0} \qquad \left[\frac{kg}{kg}\right] \tag{2}$$

where:
m_i = mass of sample at RH step i, kg
m_0 = mass of dry sample, kg

Moisture sorption was evaluated by plotting mass-related moisture content (based on each sample's lowest net weight, m_0) against RH, including standard deviations. The maximum difference between adsorption and desorption curves were calculated by subtracting desorption values from adsorption values at each humidity step. This maximum occurred at different humidities, depending on the sample: at 70% RH for uncoated paper, at 0.8 for TEOS dense, at 1:20 for TEOS:ethanol coatings, and at 80% RH for the 0.5 TEOS coating.

Water vapor diffusion resistance

Water vapor diffusion resistance of freshly coated paper samples was determined according to DIN EN ISO 12572:2017-05 by measuring the WVTR. Samples were placed in cups containing a desiccant ("dry-cup" method), and the cups were sealed in such a way that the diffusion of water vapor only took place through the sample. The cups were placed in a climatic chamber at 23°C with either 50% or 85% RH. The difference in water vapor partial pressures between the test chamber and the test vessel caused a water vapor diffusion flow through the test specimen. Cups were weighed every 90 min to calculate the WVTR, which was then used to determine the diffusion resistance μ. Each measurement was logged with weight, date, and time. The time data can be employed to ascertain the time interval between the measurement points, which is necessary to compute the water vapor diffusion flow. This is calculated in accordance with DIN EN ISO 12572 "Hygrothemal performance of building materials and products – Determination of wate vapour transmission properties – Cup method (ISO 12572:2016 + Amd 1:2024); German version EN ISO 12572:2016 + A1:2024," which is set forth in Eq. 3 as follows:

$$G = \dot{m} = \frac{m_j - m_i}{t_j - t_i} \qquad \left[\frac{kg}{s}\right] \tag{3}$$

where:
$m_{j,i}$ = measured weight at time j and i, kg
$t_{j,i}$ = time of measurement at time j and i, s

Subsequently, the water vapor diffusion flow rate can be calculated from the measured water vapor diffusion flow rate using Eq. 4:

$$g = \frac{G}{A} \qquad \left[\frac{kg}{m^2 \cdot s}\right] \tag{4}$$

where:
G = water vapor diffusion flow, kg/s
A = Area of sample, m²

Once the water vapor diffusion flow has been determined, an evaluation can be conducted. Equation 5 can be employed to ascertain the water vapor diffusion resistance number μ (μ-value):

$$\mu = \frac{\Delta p \cdot \delta_{air}}{g \cdot d} \qquad [-] \tag{5}$$

where:
d = average sample thickness, m
g = water vapor diffusion flow density, kg/(m²×s)
Δp = partial pressure difference

	Static Contact Angle, °	Specific Surface Area, m²/g
Reference (uncoated)	26 ± 12	1.7 (aged sample)
1:20 TEOS:EtOH	60 ± 5	2.9 (aged sample) 16.4*
0.5 TEOS	134 ± 3	5.2 (freshly-coated sample)
0.8 TEOS dense	111 ± 4	1.9 (aged sample)

* Literature value [14].
TEOS: tetraethoxysilane; EtOH: ethanol.

I. Static contact angle angle and specific surface area of silica-paper hybrids.

δ_{air} = water vapor diffusion conductivity coefficient of the air, kg/(m×s×Pa)

To determine the μ-value, the water vapor diffusion coefficient of the air d_{air} is required. The value is determined using Schirmer's formula (Eq. 6):

$$\delta_{air} = \frac{0{,}086 p_0}{R_D \cdot T \cdot p}\left(\frac{T}{273}\right)^{1{,}81} \quad \left[\frac{kg}{m \cdot s \cdot Pa}\right] \tag{6}$$

RESULTS AND DISCUSSION

Material characterization

The samples are characterized by static contact angle and gas physisorption measurements. The static contact angle (CA) is indicative of the wettability of the coated and uncoated samples. The highest CA was observed for the 0.5 TEOS coating (134° ± 3°), followed by 0.8 TEOS dense (111° ± 4°), and 1:20 TEOS:ethanol (60° ± 5°). Uncoated paper showed the lowest CA with (26 ± 12°). The results in **Table I** show that the uncoated paper is more hydrophilic than the coated samples, even when the high standard deviation is taken into account. The high standard deviation occurred because of fast water imbibition into the uncoated paper, making the measurement more inaccurate compared to the coated samples. Of the coated samples, 1:20 TEOS:ethanol is the most hydrophilic. The 0.8 TEOS dense and 0.5 TEOS show a hydrophobic behavior, with 0.5 TEOS being more hydrophobic compared to 0.8 TEOS dense.

The argon gas physisorption measurement showed mesopores in the 1:20 TEOS:ethanol coating with the pore size of 6 nm and a specific surface area of 2.9 m²/g on the two-year-old sample (Table I). In Mikolei et al. [14], the specific surface area of 1:20 TEOS:ethanol is mentioned with 16.4 m²/g for a freshly coated sample. A reduction in comparison to the literature value and the measured value on an aged sample are clearly seen. The reason for the reduced specific surface area might be due to aging and needs to be investigated more. The freshly prepared 0.5 TEOS coating showed mesopores with a pore size of 4 nm and a surface area of 5.2 m²/g. The hystersis, as well as the pore size distriubtion, are shown in **Figs. 2a–2b**. The 1:20 TEOS:ethanol sample and the 0.5 TEOS sample exhibit a Type IV(a) isotherm behavior. The Type IV(a) isotherm is characteristic of mesoporous materials where capillary condensation occurs with hysteresis in pores exceeding approximately 4 nm [22]. The 1:20 TEOS ethanol displays a H2(b) hysteresis loop. This type of hysteresis is typically linked to pore blocking during desorption and is associated with a narrow distribution of pore cavities combined with a wide distribution of neck sizes [22,23]. In contrast, the 0.5 TEOS coating exhibits an H3 hysteresis loop, which suggests slit-shaped mesopores [22].

The 0.8 TEOS dense sample, as well as the reference paper, shows a type II behavior of the argon physisorption isotherms (Figs. 2c–2d). This indicates that the silica coating 0.8 TEOS dense is predominantly nonporous or microporous in nature [22,23]. The 0.8 TEOS dense has a surface area of 1.9 m²/g. The reference paper has a surface area of 1.7 m²/g. The results are summarized in Table I.

Water vapor sorption of different silica-coated cotton linter papers

Figure 3 demonstrates the sorption isotherms of uncoated paper and the coated papers. It shows the change in mass vs. RH. The change in mass is expressed as a mass percentage of the lowest measured weight of the respective sample (measured at 0% RH). Consequently, 0% RH represents the zero point of the isotherm.

As shown in Fig. 3, the change in mass in relation to the RH is clearly visible. The coated papers show reduced mass change, demonstrating the influence of functionalization on water vapor uptake. A closer look on the coating compositions reveals a correlation between the uptake of moisture, the specific surface area, and the hydrophobicity. The 1:20 TEOS:ethanol and 0.5 TEOS both have integrated mesopores shown by the argon measurement. They also differ in the ratio of non-polar groups and the hydrophobicity shown by CA-measurements. For comparing the specific surface area of the freshly coated samples, the literature value [14] for the 1:20 TEOS:ethanol coating is used, while the value for the 0.5 TEOS coating is derived from argon gas physisorption measurements. Additionally, to the lower surface area, the 0.5 TEOS coating is significantly more hydro-

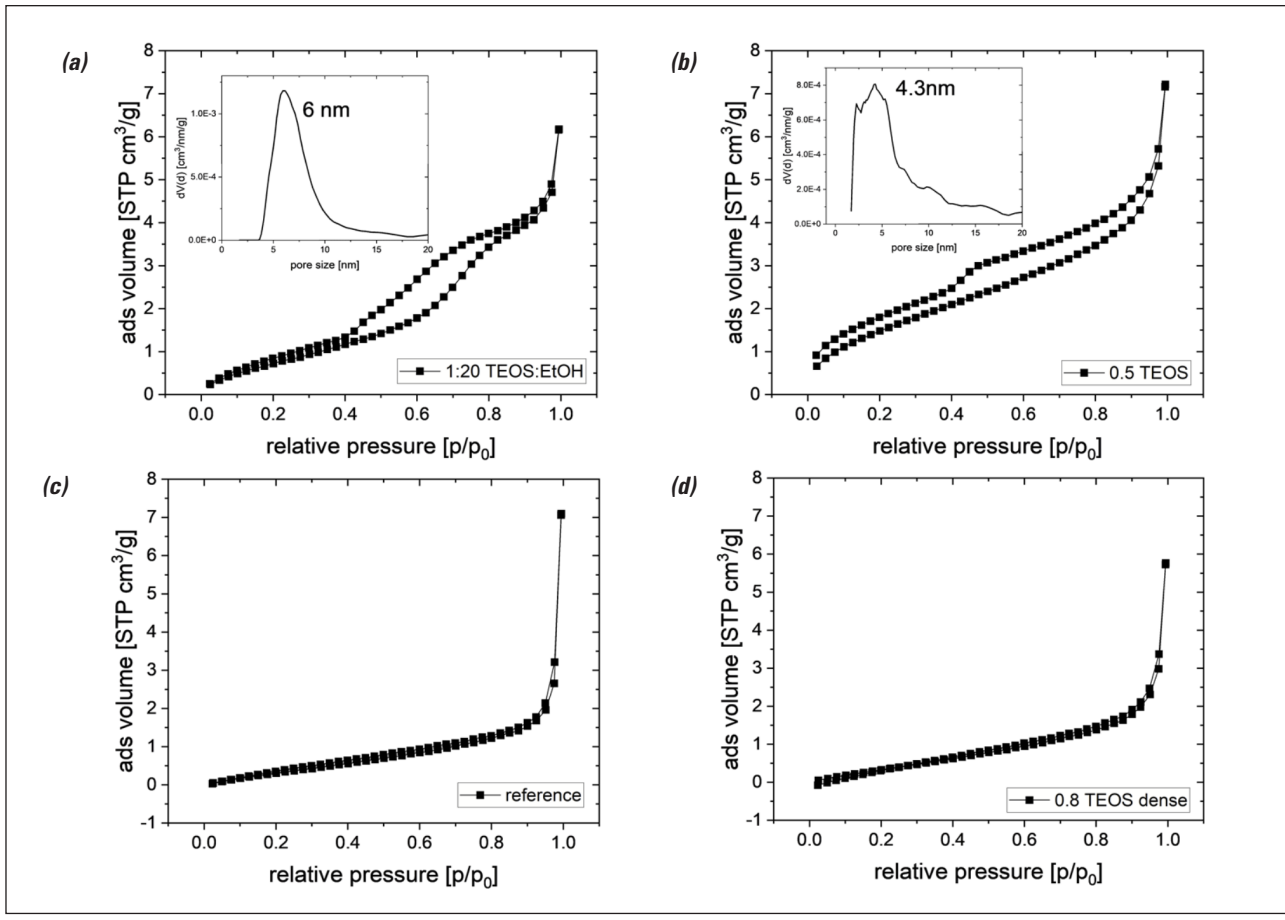

2. Argon physisorption isotherms for the silica-paper hybrid materials. (a) 1:20 tetraethoxysilane (TEOS):ethanol (EtOH) coating, 2-year-old samples; (b) 0.5 TEOS coating, freshly coated samples; (c) uncoated paper, 2-year-old samples; and (d) 0.8 TEOS dense coating, 2 year-old-samples (ads: adsorbed; STP: standard temperature and pressure; p/p_0: ratio of equilibrium gase, p, to saturation vapor pressure, p_0).

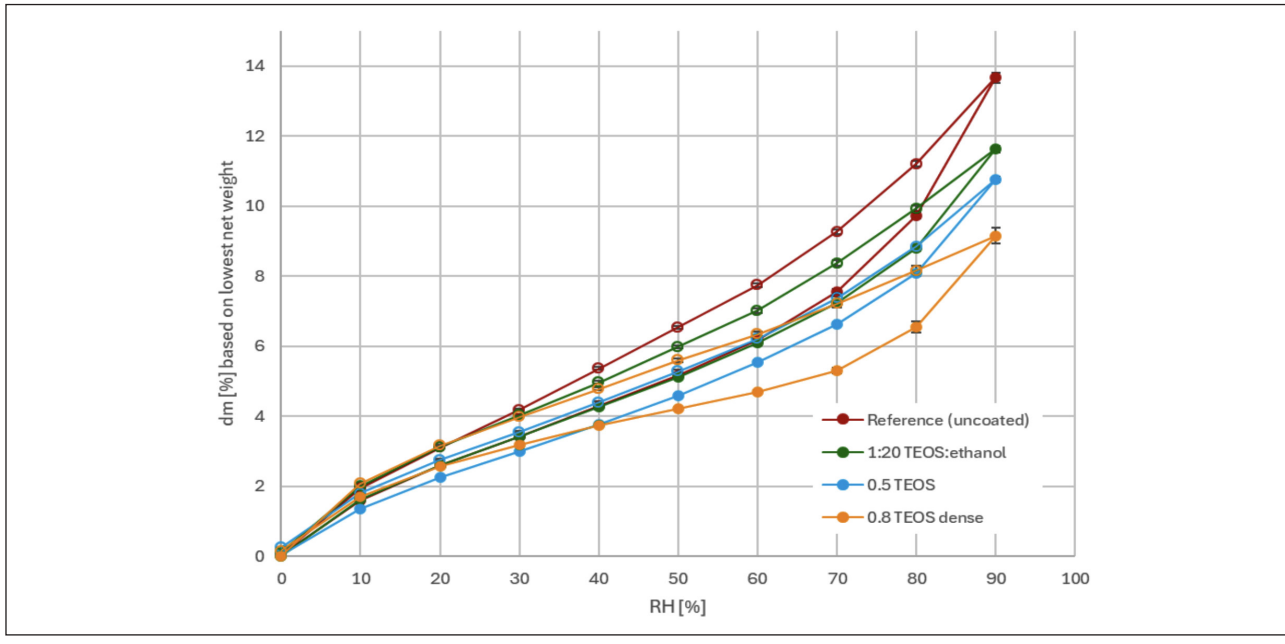

3. Change in mass (dm) over vapor (relative humidity, RH); average values. Colored data points for adsorption; hollow data points for desorption.

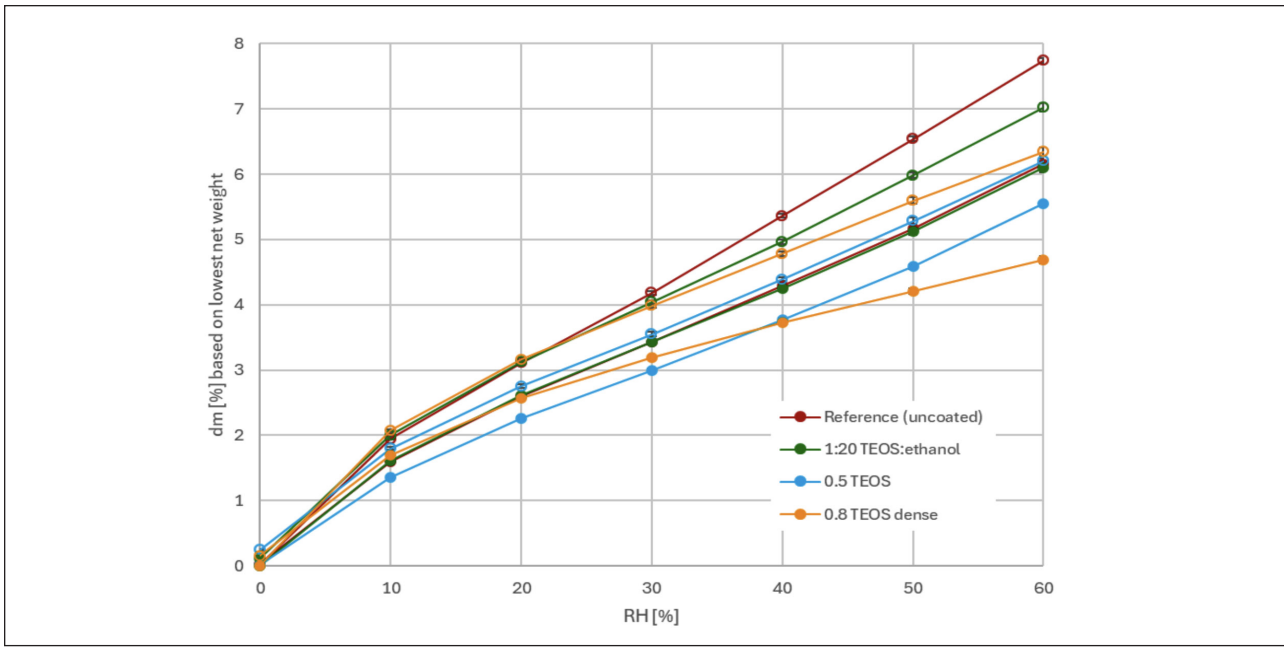

4. Change in mass over vapor in the range of 0–50% RH; average values. Colored data points for adsorption; hollow data points for desorption.

phobic (comparison CA) compared to the 1:20 TEOS:ethanol. The higher adsorption of water vapor of the 1:20 TEOS:ethanol compared to the 0.5 TEOS could be due to the higher hydrophilic behavior, as well as the bigger specific surface area of freshly coated samples.

A comparison between the 0.5 TEOS and 0.8 TEOS dense coatings also reveals some insightful results. The 0.5 TEOS coating has mesopores embedded in the coating, whereas the 0.8 TEOS dense coating does not. The 0.8 TEOS dense variant exhibits a higher TEOS ratio and a lower non-polar group ratio in comparison to the 0.5 TEOS variant, which also influences the static contact angle measurements that show a small difference between 0.5 TEOS and 0.8 TEOS dense in the wettability of the surface. A CA of 134° is found in 0.5 TEOS, and in 0.8 TEOS dense, a CA of 111° was measured.

Up to a 40% RH, the mass change of the 0.5 TEOS coating is lower than that of the 0.8 TEOS dense coating. However, above 40% RH, the mass change of the 0.5 TEOS coating exceeds that of the 0.8 TEOS dense coating (see **Fig. 4**). This might be attributed to the presence of mesopores in the 0.5 TEOS coating. In his work, Funk [24] outlines the vapor ranges in which mesopores in porous materials adsorb moisture, and he specifically addresses the mechanism of moisture adsorption by mesopores. Funk's research clearly shows that mesopores adsorb moisture at 35%–92% RH via surface and capillary condensation. The mass change of the 0.5 TEOS coating, initially lower at up to 40% RH, then rises to a higher mass change at 40% RH. This is well within the range defined by Funk, indicating water adsorption in the mesopores. The specific surface area and pore size of the individual coatings measured will provide valuable insight into this phenomenon. Another indication of water absorption in the mesopores is based on Mikolei et al. [15]. Mikolei et al. performed a sorption measurement for the 1:20 TEOS:ethanol coating, and small angle X-ray scattering (SAXS) was used to observe the uptake of water vapor in the mesopores. The uptake of water vapor inside of the mesopores started, as deduced by a Bragg peak, at 50% RH. The mesopores were observed to be completely filled at 90% RH, resulting in an almost complete disappearance of the Bragg peak. This finding suggests that the lower mass change under 40% RH of the 0.5 TEOS might be associated with the mesopores, which are also integrated into the 1:20 TEOS:ethanol coating used in the study with the SAXS. In addition, it is important to investigate whether the lower mass change at relative humidities below 40% RH is related to the higher non-polar fractions of the 0.5 TEOS coating compared to the 0.8 TEOS dense coating. This can be verified by varying the non-polar content and conducting additional sorption measurements.

It is evident that hysteresis is present in all measurements and manifests itself to varying degrees (Fig. 3). Hysteresis can be defined as a slight deviation of the adsorption and desorption curves. The confirmation of hysteresis is supported by the number of samples and the low maximum standard deviation that occurred, which allows for the reproducibility of the results.

In order to determine the maximum difference between the adsorption and desorption of a coating, the difference in mass change was calculated for the vapor with the maximum discrepancy between the adsorption and desorption curves. The maximum deviations observed in the coating samples vary considerably. The 0.8 TEOS dense coating

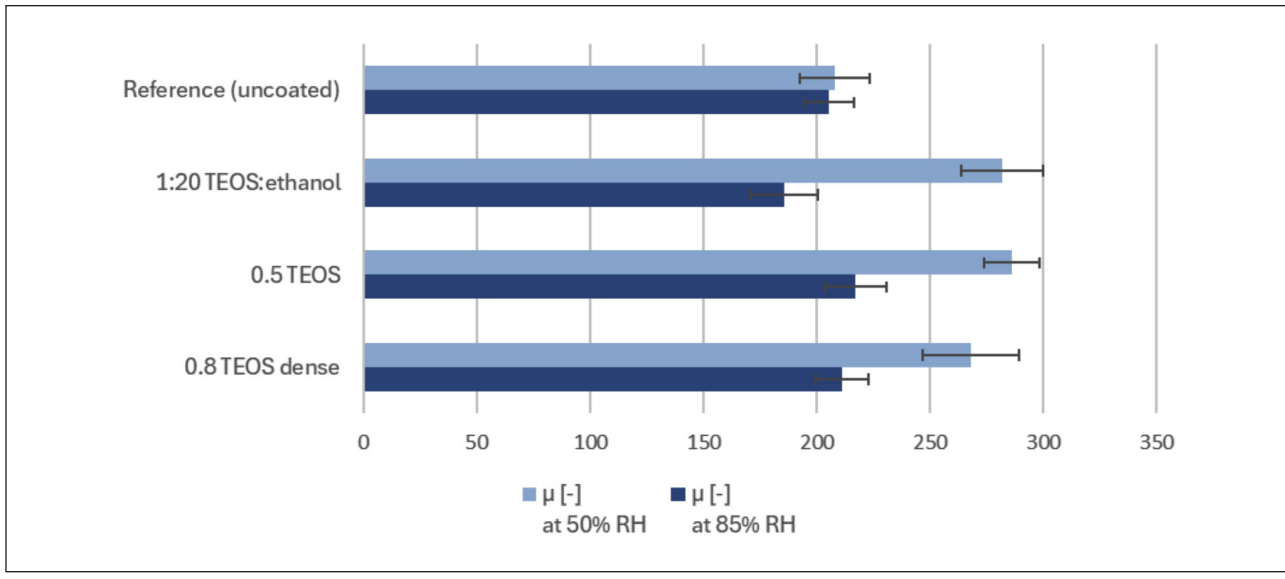

5. Water vapor diffusion resistance number, μ, of an uncoated linter paper and different silica-coated linter papers.

demonstrates the highest maximum difference at 1.91 mass%, while the reference paper exhibits the second highest difference at 1.71 mass%.

The 1:20 TEOS coating demonstrates a maximum difference of 1.14 mass%, and the 0.5 TEOS coating exhibits the lowest maximum deviation between the adsorption and desorption curves. The maximum deviations of the hysteresis are summarized in **Table II**. Hysteresis, a well-known phenomenon in hygroscopic materials, arises from the different behavior of water adsorption and release. The hysteresis of the water-vapor physisorption isotherm represents energy dissipated due to irreversibility, which is generally attributed to underlying retention forces or pore-blocking ("ink-bottle") effects within the material's microstructure and nanostructure. These effects cause desorption to be less reversible and to require additional energy input to release stored water, as discussed in mechanistic analyses of wood and other porous building materials [25-28]. A larger hysteresis in wood or other hygroscopic materials corresponds to greater energy dissipation during adsorption-desorption cycles, reflecting stronger retention forces or pore-blocking effects in the microstructure. Conversely, a smaller hysteresis is generally associated with more reversible water release and reduced energy loss, meaning that materials with narrower hysteresis loops tend to facilitate easier drying or "superior" water release under equilibrium conditions [26,29].

	Maximum Hysteresis, mass%
Reference (uncoated)	1.71
1:20 TEOS:EtOH	1.14
0.5 TEOS	0.77
0.8 TEOS dense	1.91
TEOS: tetraethoxysilane; EtOH: ethanol.	

II. Maximum difference between adsorption and desorption curves.

In comparison to the 0.8 TEOS dense coating without mesopores, the incorporation of mesopores into the 1:20 TEOS and 0.5 TEOS coatings has been shown to increase the samples' specific surface area as deduced from the argon gas physisorption measurement. This has the potential to result in divergent water adsorption and release behaviors. A comparison of the 1:20 TEOS and 0.5 TEOS coatings with the reference paper reveals a reduced maximum difference between adsorption and desorption curves. This confirms that the mesopore coatings facilitate superior water release compared to the reference paper.

As Mikolei et al. [13] state, water is absorbed at a faster rate when mesoporous coatings are used than when uncoated paper is used. The investigation of water release was not within the scope of the study. However, the results of the physisorption measurement in the present study indicate that there is an additional, favored release of water. This finding lends further credence to the hypothesis that the mesopore coatings facilitate superior water release in comparison to the reference paper.

Water vapor diffusion resistance of silica-coated cotton linter papers

Figure 5 shows the calculated water vapor diffusion resistance number of a reference (uncoated) and different coated paper specimens. The higher the value, the higher the material's ability to resist water vapor diffusion compared to a static air layer. The results show a correlation between the water vapor diffusion resistance of silica-coated paper and vapor. In the case of the uncoated paper, no such dependency is evident. The water vapor diffusion resistance

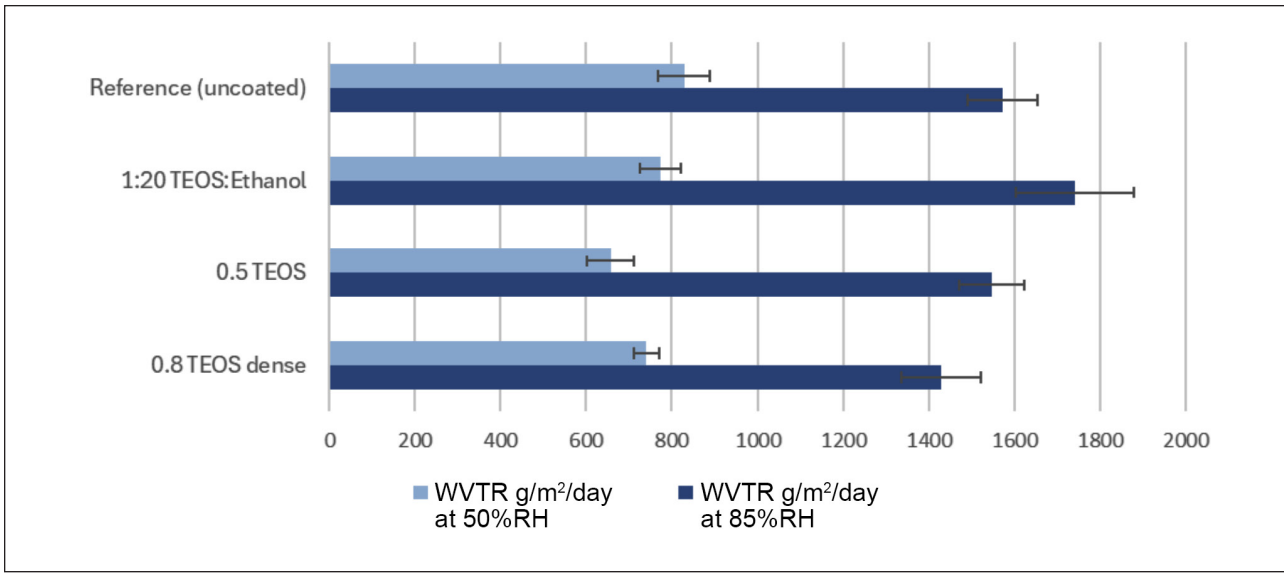

6. Water vapor transmission rate (WVTR) of uncoated and coated linter papers.

of the coated paper is observed to be higher at a condition of 50% RH (light blue) in comparison to a condition of 85% RH (darker blue).

Figure 6 substantiates these results. It shows the water vapor transmission rate in grams per square meters per day (g/m²/day) for the uncoated reference paper and the different coated paper specimens. Unlike the water vapor diffusion resistance (μ), this analysis does not take ambient air pressure into account, which is why the difference between the values measured at 50% RH (light blue bars) and 85% RH (dark blue bars) is significantly higher. The standard deviation of the measured values is < 5% for all samples, except for the 1:20 TEOS:ethanol measured at 85% RH (>7%), and thereby complying with the DIN EN ISO 12572.

The results for the coated papers demonstrate their initial suitability for further development as moisture-variable vapor barriers. Comparing our results to the performance of conventional variable vapor barriers (Fig. 1), our laboratory measurements on silica-coated linter papers show a qualitatively similar trend; a higher vapor is accompanied by significantly lower water vapor resistance in the material (Fig. 5). This confirms that functionalized paper can reproduce the moisture-dependent diffusion behavior essential for adaptive vapor barriers in building physics.

In order for the coatings to be utilized as a moisture-variable vapor barrier, it is essential that the resistance increases at lower relative humidities. In the work of Bosse [30], the minimum s_d-values for damage-free insulated roofs and internally insulated walls are provided. For internally insulated walls, the range is between 0.65 m and 4 m. The 0.65 m value is applicable in conditions of high vapor, while the 4 m value is applicable in conditions of low vapor. For the roof construction, the value was determined to be between 0.27 m and 7 m. In order to employ coated papers as a moisture-variable vapor barrier within a building construction, the μ-value must be between approximately 5,150– 31,700 or 2,140–55,500. The μ-values can vary slightly depending on the thickness of the material. Given its status as a foil, it is expected that the thickness will remain within a low range. Consequently, the water vapor diffusion resistance must be elevated (see Eq. 1). However, it is evident that the existing results are not yet commensurate with these values. It is imperative that the coatings are developed to be more impermeable to water vapor diffusion at both low and high relative humidities, while maintaining the proven moisture variability.

CONCLUSION

This study examined the potential of silica-coated papers for use as a moisture-variable water vapor barrier. Such an application is considered to represent a more sustainable alternative to conventional materials used in the construction industry, such as polyamide, for example.

The results demonstrated that the coating of the papers can influence the water vapor permeability and the adsorption and desorption behavior in comparison to uncoated papers. The coatings with mesopores and those without exhibited distinct differences in their physisorption behavior. The dense coating with 0.8 TEOS demonstrated slightly reduced mass changes upon water adsorption at high humidity levels in comparison to uncoated paper under the applied conditions. However, further investigation is required to elucidate the phenomenon of hysteresis or to develop strategies to increase the water volume uptake.

The results of the water vapor diffusion resistance indicate a correlation with the relative humidity and therefore the vapor pressure. The coated papers demonstrate an enhanced water vapor diffusion resistance at lower humidity levels. At higher relative humidities, a decrease in water vapor diffusion resistance has been observed. This phenomenon is also pres-

ent in the case of moisture-variable vapor control layers in the building industry. While these outcomes are encouraging, the study also identifies several areas that require refinement of the coatings. The silica-paper hybrids investigated in this study have yet to demonstrate the requisite water vapor diffusion resistance for practical application in moisture-sensitive structures, such as insulated roofs and internally insulated walls. Future work will focus on an enhancement of the water vapor diffusion resistance of these coatings while preserving their moisture variability.

In conclusion, silica-coated papers show great promise as moisture-variable vapor control layers. However, further research is necessary to optimize their performance characteristics and ensure that they meet the practical requirements for widespread use in the construction industry.

This research constitutes a vital preliminary step in the development of more sustainable and recyclable vapor control layer materials, with the objective of reducing reliance on fossil-based polymers in the construction industry.

ACKNOWLEDGEMENTS

The authors would like to thank Joanna J. Mikolei and Dominik Richter for their support in producing the coatings and to Markus Biesalski for their kind permission to utilize the laboratory facilities (Technical University of Darmstadt, Smart Membranes & Macromolecular Paper Chemistry). In addition, the authors would like to thank Christiane Helbrecht and Samuel Schabel for their support in the paper production process (Technical University of Darmstadt, PMV).

LITERATURE CITED

1. Sununta, S., Rattanarat, P., Chailapakul, O., et al., *Anal. Sci.* 34: 109(2018). https://doi.org/10.2116/analsci.34.109.
2. Li, Z., Yi, Y., Luo, X., et al., *J. Med. Virol.* 92(9): 1518(2020). https://doi.org/10.1002/jmv.25727.
3. Lee, H.M., Choi, S.-Y., Jung, A., et al., *Angew. Chem., Int. Ed.* 52(30): 7718(2013). https://doi.org/10.1002/anie.201301941.
4. "Leitfähiges Papier SmartFeel®" ["SmartFeel® conductive paper"], *Heating Solutions*, Papierfabrik Louisenthal GmbH, Gmund am Tegernsee, Germany. Available [Online] https://www.louisenthal.com/solutions/industry/heating-solutions <12March2025>.
5. "Technischer Fortschritt bei Papier: Neue Barrierequalität flexibler Verpackungen durch Dispersionsveredelung [Technological progress in paper: New barrier quality for flexible packaging through dispersion finishing"], Industrieverband Papier- und Folienverpackung e.V. Technischer Fortschritt bei Papier [German Association of Paper and Film Packaging Manufacturers — Technical Progress in Paper], Berlin, 31 January 2020. Available [Online] https://ipv-verpackung.de/2020/01/31/technischer-fortschritt-bei-papier-neue-barrierequalitaet-flexibler-verpackungen-durch-dispersionsveredelung/ <12March2026>.
6. Kopacic, S., Walzl, A., Zankel, A., et al., *Coatings* 8(7): 235(2018). https://doi.org/10.3390/coatings8070235.
7. Lee, M., Kim, S., Kim, H.-Y., et al., *Phys. Fluids* 28(4): 042101(2016). https://doi.org/10.1063/1.4944659.
8. Samyn, P., *J. Mater. Sci.* 48(19): 6455(2013). https://doi.org/10.1007/s10853-013-7519-y.
9. Bedane, A.H., Eić, M., Farmahini-Farahani, M., et al., *J. Membr. Sci.* 493: 46(2015). https://doi.org/10.1016/j.memsci.2015.06.009.
10. Knaack, U., Bach, R., and Schabel, S., Eds., *Bauen mit Papier. Architektur und Konstruktion [Building with Paper: Architecture and Construction]*, Birkhäuser Verlag, Basel, 2023.
11. Dubois, C., Herzog, N., Rüttiger, C., et al., *Langmuir* 33(1): 332(2017). https://doi.org/10.1021/acs.langmuir.6b03839.
12. Nau, M., Herzog, N., Schmidt, J., et al., *Adv. Mater. Interfaces* 6(18): 1900892(2019). https://doi.org/10.1002/admi.201900892.
13. Mikolei, J.J., Neuenfeld, L., Paech, S., et al., *Adv. Mater. Interfaces* 9(19): 2200064(2022). https://doi.org/10.1002/admi.202200064.
14. Mikolei, J.J., Richter, D., Pardehkhorram, R., et al., *Nanoscale* 20: 9094(2023). https://doi.org/10.1039/D3NR01247F.
15. Mikolei, J.J., Biesalski, M., Ceolin, M., et al., *Cellulose* 31(9): 5855(2023). https://doi.org/10.1007/s10570-024-05945-2.
16. Mikolei, J.J., Stanzel, M., Pardehkorram, R., et al., *Adv. Mater. Interfaces* 10(21). 2300211(2023). https://doi.org/10.1002/admi.202300211.
17. "Process data set: Vapor barrier PE," *ÖKOBAUDAT* [Ecological Construction Material Database], Bundesministerium für Wohnen, Stadtentwicklung und Bauwesen [Federal Ministry for Housing, Urban Development and Construction], Berlin. Available [Online] https://www.oekobaudat.de/OEKOBAU.DAT/datasetdetail/process.xhtml?lang=de&uuid=7b949ae4-3793-4670-86d8-241578803aa2&version=20.21.060 <12March2026>.
18. Karali, N., Khanna, N., and Shah, N., "Climate impact of primary plastic production," OSTI ID: 2336722, Lawrence Berkeley National Laboratory, Berkely, CA, USA, 2024. Available [Online] https://escholarship.org/uc/item/6cc1g99q <12March2026>.
19. Beyler, C.L. and Hirschler, M.M., "Thermal decomposition of polymers," in *SFPE Handbook of Fire Protection Engineering*, Society of Fire Protection Engineers/National Fire Protection Association, Qunicy, MA, USA, 2002.
20. Olaoye, T.S., Dewsbury, M., and Künzel, H., *Energies* 14(13): 4053(2021). https://doi.org/10.3390/en14134053.
21. "DB+ Armierte Hydrosafe ® Dampfbremse aus Baupappe" ["DB+ Reinforced Hydrosafe® vapor barrier made of construction paper"], Technical Data, ProcClima, Schwetzingen, Germany. Available [Online] https://de.proclima.com/produkte/dichtung-innen/dbplus/technische-daten#sub_navigation <12March2026>.

ABOUT THIS PAPER

Cite this article as:
Bosse, N., Czerwenka, L., Andrieu-Brunsen, A., et al., *TAPPI J.* 25(3): 169(2026).
https://doi.org/10.32964/TJ25.3.169

DOI: https://doi.org/10.32964/TJ25.3.169

ISSN: 0734-1415

Publisher: TAPPI Press

About this journal

22. Thommes, M., Kaneko, K., Neimark, A.V., et al., *Pure Appl. Chem.* 87(9-10): 1051(2015). https://doi.org/10.1515/pac-2014-1117.

23. Schlumberger, C. And Thommes, M., *Adv. Mater. Interfaces* 8(4): 2002181(2021). https://doi.org/10.1002/admi.202002181.

24. Funk, M., "Hysteresis der Feuchtespeicherung in porösen Materialien" ["Hysteresis of moisture storage in porous materials"], Ph.D. dissertation, Technical University of Dresden, Dresden, Germany, 2012.

25. Fredriksson, M., *Forests* 10(9): 779(2019). https://doi.org/10.3390/f10090779.

26. Fredriksson, M. and Thybring, E.E., *PloS One* 14(11): e0225111(2019). https://doi.org/10.1371/journal.pone.0225111.

27. Pinson, M.B., Masoero, E., Bonnaud, P.A., et al., *Phys. Rev. Appl.* 3(6): 064009(2015). https://doi.org/10.1103/PhysRevApplied.3.064009.

28. Pöllmann, A., Reinelt, M., and Briesen, H., *Materials* 15(17): 6031(2022). https://doi.org/10.3390/ma15176031.

29. Lang, Q., Biziks, V., and Militz, H., *Forests* [Online] 2023, 14(10): 2015(2023). https://doi.org/10.3390/f14102015.

30. Bosse, N., "Untersuchung der bauphysikalischen Leistungsfähigkeit funktionalisierter Papiere im hygroskopischen Feuchtebereich" ["Investigation of the building physics performance of functionalized papers in the hygroscopic humidity range"], Master's thesis, Technical University of Darmstadt, Darmstadt, Germany, 2024.

ABOUT THE AUTHORS

Bosse

Czerwenka

Andrieu-Brunsen

Bishara

The building sector has one of the highest CO_2 emissions in the world. In our research group (Paper Construction and Design), we try to implement paper in the building sector. Our goal is to use the given or functionalized properties of paper-based materials for load bearing, insulation, or protective layers against humidity/weathering. Due to the high recyclability of paper, paper-based materials are a great material to subsitiute for traditonal materials in the building industry.

This research complements the research already being done on these coatings in the Chemistry Department at the Technical University of Darmstadt. So far, only fluid transport, as well as a sorption measurement, on one coating has been done. In the current research, the sorption measurement is complimented with other coatings, and a water vapor diffusion resistance is determined for two different relative humidities.

The most difficult aspect of this research was to find a suitable test setup to determine the water vapor diffusion resistance of the samples. Initially, there were many influencing factors that distorted the result. The solution was to use a standard with correction factors for various influences. A standard from the construction industry was very helpful here.

It was interesting to discover that the silica paper hybrids have a different water vapor diffusion resistance depending on the relative humidity of the sample, as uncoated paper does not show this effect. The water vapor diffusion resistance is higher at lower relative humidities than at higher relative humidities. In the construction industry, this effect is used as a moisture-dependent water vapor barrier to protect a building component from moisture.

Once the moisture-variable water vapor barrier is developed, mills can use this information to expand their products into the building industry sector. Mills can provide the paper as a basis for the silica-paper hybrids to develop innovative, high-performance building materials meeting the demand for sustainable and advanced construction solutions.

The research shows very good initial findings and effects in the silica-paper hybrids. However the coatings need to be optimized to ensure a higher water vapor diffusion resistance. Right now, it is not high enough to be used as a water vapor barrier. The next step is to optimize the coating to make it more water vapor tight while maintaing the characteristics of a higher water vapor diffusion resistance at lower relative humidities compared to higher relative humidities.

Bosse is a research assistant and Bishara is a post-doctoral researcher at the Institute of Structural Mechanics and Design, Department of Civil and Environmental Engineering, Technical University of Darmstadt, in Darmstadt, Germany. Bishara is also a professor of Building Systems and Building Simulation in the School of Engineering, Civil Engineering and Sustainability, at Mainz University of Applied Sciences in Mainz, Germany. Czerwenka is a research assistant and Andrieu-Brunsen is a professor in the Macromolecular Chemistry-Smart Membranes Group, Ernst-Berl Institute for Technical and Macromolecular Chemistry, at the Technical University of Darmstadt, in Darmstadt, Germany. Email Bosse at bosse@ismd.tu-darmstadt.de.